

Block-copolymer directed *in-situ* synthesis of Mesoporous SiCN and Supported Au & Ag nanoparticles for Catalysis

Saravanakumar Thayuman,^[a] Winfried Kretschmer,^[a] and Gunter Mötz,^[b]

[a] Prof. Dr. Rhett Kempe,
Lehrstuhl Anorganische Chemie II,
Universität Bayreuth,
95440 Bayreuth, Germany,
e-mail : saravanakumar.thayuman@gmail.com

[b] Lehrstuhl Keramische Werkstoffe,
Universität Bayreuth,
95440 Bayreuth, Germany.
e-mail : guenter.motz@uni-bayreuth.de

Supporting information for this article is given via a link at the end of the document.

Abstract: Novel concerted copolymerization, microphase separation, and crosslinking strategy for the synthesis of mesoporous SiCN with high surface area has been developed. Influence of pore size and surface area by changing length and ratio of *porogen* organic block is demonstrated. Longer the chain length and higher the porogen ratio trends the SiCN under mesoporous region with high surface area. Whereas shorter chain length porogen trends the SiCN under microporous region. The de Boer method, Brunauer–Emmett–Teller (BET), and statistical thickness plot (t-plot) are utilised to confirm mesoporous and microporous textural properties of the SiCN. The same synthetic strategy is also extended to the synthesis of mesoporous SiCN supported metal nanoparticles. Well distributed *in situ* formation of gold and silver nanoparticles during the synthesis of mesoporous SiCN is emerged followed by successful prevention of sintering at 1000°C. Synthesized materials are mainly characterized by transmission electron microscopy, scanning electron microscopy, atomic force microscopy, powder X-ray diffractometer and nitrogen physisorption techniques.

Introduction

Polymer-derived ceramics (PDCs) have gained significant attention in the field of aerospace components, battery electrode, and catalysis due to their unique combination of thermal stability, mechanical strength, and tuneable porosity.^[1] Particularly mesostructured PDCs and their textural properties are inevitable as catalyst support in catalysis because mesoporous supports, for instance, have many additional features such as stabilization of nanoparticles and selective transport of substrates^[2]. Within the PDCs classifications, non-oxide supports, porous siliconcarbonitride (SiCN), is recently used as solid support for transition metal nanoparticles to study wide range of catalysis.^[3] Reportedly, the porosity is introduced to SiCN supported nanoparticles system by polystyrene template or organic *porogen* polymers. Wiesner and coworkers have pioneered that platinum nanoparticles can be formed *in-situ* during the synthesis of mesoporous SiCN using lithographic micromolding and multicomponent self-assembling procedure.^[4] This work is indeed the frontier piece in the field of non-oxide ceramic

supported metal nanoparticle. The produced SiCN support is well ordered and over the 100 nm pore size pores. This process implies that the platinum precursor binds selectively to the polymer derived ceramic precursor and self-assembling takes place in the presence of organic copolymer that acts as a structural directing agent. This work is indeed the frontier piece in the field of non-oxide ceramic supported metal nanoparticle. However, the synthesis required multi-steps and sophisticated laboratory environment with well-equipped instruments. Later on, Kempe group have emphasized the selective functional group binding of metal complex on ceramic precursor followed by transmetallation reaction leading to the synthesis of nickel nanoparticles supported microporous SiCN.^[5] Availability of pores in the mesoscale is important to have pronounced permeability and molecular diffusion for better catalytic performance.^[6] It is required to have support in mesoscale possessing high surface area as well as metal particles in nanoscale and not blocking the pores. Notably, Polystyrene template directed synthesis of mesoporous SiCN is recently reported by Kempe and Motz group with surface area of 110 m²/g.^[7]

Alternative to template directed approach, single pot synthesis of inorganic-organic block copolymerization approach is drawn substantial attention for the synthesis of mesoporous SiCN.^[8] This single step copolymerization approach is promising in the way that the resultant SiCN is expected to be a mesoporous material since the blocks are covalently linked and undergo microphase separation in mesoscale.^[9] Top of all, the metal precursor binds selectively to the inorganic block that induces transmetallation during self-assembly. Recently, the synthesis of SiCN nanofibers adopting concerted copolymer formation, microphase separation, and crosslinking process is communicated as a promising procedure for the synthesis of mesostructured materials.^[10] Polyethylene with hydroxyl end group (PE-OH) synthesised by Ziegler's "Aufbaureaktion"^[11] and polymeric ceramic carbosilazane precursor (PCCP) are used as organic and inorganic blocks respectively.

Here in this report the synthesis of solid mesoporous SiCN support with highest surface area of 460 m²/g via concerted copolymer formation, microphase separation, and

pyrolysis at high temperature. Also variation in pore size and surface area is observed as altering the length and ratio of organic *porogen* block. The report also includes gold and silver nanoparticles supported mesoporous SiCN synthesized at 1000°C. Mesoporous non oxide support in mesoscale (2-50 nm) containing metal nanoparticles is not reported to the best of our knowledge. The synthesized metal nanoparticles containing samples were possessing high surface area of 206-303 m²/g. Controlled pyrolysis of these morphologies result mesoporous SiCN support. The morphology of the support and its textural properties such as surface area, size of the pores play a key role in catalysis. Thus the mesoporous SiCN support was first optimized by tuning the type of porogen blocks and the length of the porogen blocks before introducing metal particles to ensure the support was with high surface area and in the mesoscale range. As the length of organic block increases, pore size and volume increased. While ratio of organic block increases, the surface area of mesoporous SiCN increased in the outcome. The synthesized support is mainly characterized by nitrogen physisorption, transmission electron microscopy (TEM) and scanning electron microscopy (SEM).

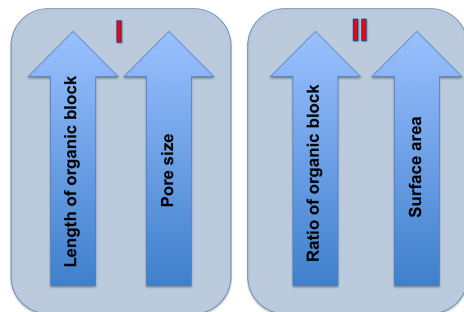


Figure 1. Observed textural properties of the as synthesised materials. I. Length of the organic block increases, pore size increases. II. Weight ratio of organic block increases, surface area of resultant SiCN is increased.

Results and Discussion

Inorganic and crosslinkable PCCP with different ratio were added to pore generating PE-OH and green-bodies of PEOHTT-1 (30:70) and PEOHTT-2 (70:30) were synthesized via concerted solvent casting, melt annealing and crosslinking technique (Fig. 3). The PEOHTT-2 green body is chosen for the AFM analysis to figure out the morphology exist in the sample which shown a new type of segregated morphology (Fig. 5. a&b). After pyrolysing the green bodies, mesostructured SiCN if obtained and subsequently the physisorption studies were carried out to the resultant SiCN-1 from greenbody PEOHTT-1 and SiCN-2 from greenbody PEOHTT-2 (Fig. 3). The highest surface area of 460 m²/g was observed on SiCN-2 sample with the pore size distribution of 9.31 nm (Tab. 1). Whereas, SiCN-1 sample have shown the surface area of 117 m²/g with the pore size congruent to SiCN-2 sample (Tab. 1). This result inferences that the lower ceramic precursor content is preferable to achieve SiCN with high surface area due to the larger quantity of void space left by PE block and SiCN surface exposure to the physisorption (Fig. 3).

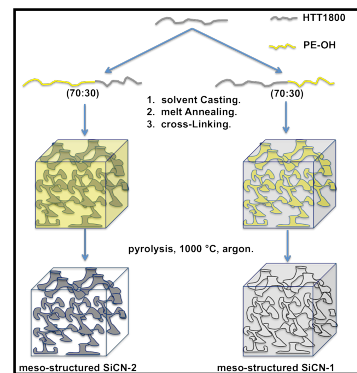


Figure 3. The schematic diagram describing the synthetic route to mesoporous SiCN support.

In parallel, short chain alcohol, unilene 700 alcohol, was examined with same PCCP to study the change in textual properties as length of the alcohol is decreased. Green bodies of UniOHTT-3 and UniOHTT-4 are prepared by similar concerted procedure and then pyrolysed at 1000°C under inert atmosphere. The SiCN-3 and SiCN-4 sample, obtained from PEOHTT-3 and PEOHTT-4 respectively, were analyzed by physisorption method with exhibiting high surface area for the sample SiCN-4 with 383 m²/g with pore size distribution of 1.3 nm. Outcome of this experiments attributes the shorter chain alcohol induces micropores and longer chain PE-OH influences mesopores. This results were confirmed by the physisorption and WXRD analysis.

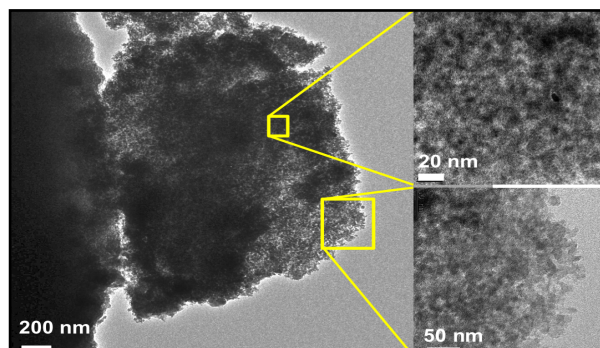


Figure 3. Representative TEM image (200 nm scale) of mesoporous SiCN-2 with magnified inset (20&50 nm scale).

Firstly change of weight ratio is experimented for the improvement in surface area. The sample SiCN-1, having 30% of PE block, exhibits with surface area of 117 m²/g and pore volume of 0.124 cc/g. On the other hand, the highest BET surface area of 460 m²/g was observed for SiCN-2, having 70% of PE block, with pore size distribution that solely belongs to mesoscale (9.414 nm). The large quantity of void space was substantiated from the calculated adsorbed pore volume of 0.553 cm³/g. This implies that increasing the weight fraction of PE introduces large quantity of void space in the sample that leading to mesoporous SiCN with highest surface area.

Secondly, we were curious to know if the length of the alcohol brings any changes in the pore size. Interestingly, Sample SiCN-4, having 70% of unilene alcohol, was observed to have pores predominantly in microscale with total BET surface area of 383 m²/g and pore size distribution of 1.379

nm. A similar trend is observed for the sample SiCN-3 with surface area 236 m²/g and and pore size distribution of 1.289 nm. Furthermore, The de Boer method is widely used to calculate the surface area and pore volume for exclusively microporous materials.^[12] The sample SiCN-4 shown 328 m²/g with micropore volume of 0.166 cc/g and sample SiCN-3 shown 220 m²/g and 0.130 cc/g. Additionally, a critical evaluation using statistical thickness plot (t-plot)^[13] was performed to understand more about the porous nature of all the samples. Interestingly, calculated positive intercept for SiCN-3 and SiCN-4 samples and negative intercept (extrapolated to zero) for SiCN-1 and SiCN-2 samples confirms the presence of micropores in SiCN-3 and SiCN-4 (fig.7) samples. Allover again, a typical mesoporous material attributed type of IV isotherm observed for SiCN-1 (PEOHTT-1) and SiCN-2 (PEOHTT-2), Whereas for SiCN-3 (UniOHTT-1), SiCN-4 (UniOHTT-2) samples shown type II isotherm that is countable for micropores.

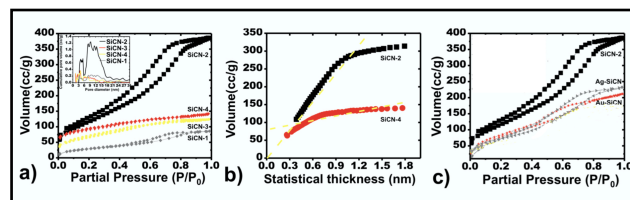


Figure 6. a) Stacked hysteresis of the SiCN-1, SiCN-2, SiCN-3 and SiCN-4 with the inset of respective stacked pore size distribution. b) The v-t plot study of SiCN-2 and SiCN-4 samples. c) Stacked hysteresis of the SiCN-2, Au@SiCN and Ag@SiCN.

In order to continue with the preparation of metal containing SiCN, we preferred adapting with sample preparation procedure of SiCN-2 because of the fact that mesoporous materials in comparison with microporous have many additional features for the catalytic application.^[14] Among wide library of metal complexes to be chosen as precursor for the formation of nanoparticles, aminopyridinato complexes^[15] were chosen because these metal complexes claim to have many unique property of binding selectively on PCCP block. Apart from binding covalently with amino and silyl functional groups of PCCP block, these aminopyridinato complexes are also capable of undergoing transmetallation reaction as well as increasing the yield of the final ceramics. Gold and silver aminopyridinato complexes were synthesized as reported and injected to the solution of PCCP and PE-OH. Following with the copolymer formation, microphase separation, and crosslinking process, green bodies of respective metal complex with copolymer of PCCP and PE-OH were pyrolysed at 1000°C. It is well known that the structural deformation or phase transformation of support^[16] and sintering of nanoparticles^[17] to take place upon heating the green body at high temperature. Non-oxide ceramic support was chosen to overcoming both structural deformation of support as well as resisting to sintering of supported nanoparticles.^[18] Coinage nanoparticles are chosen to have on these novel mesoporous SiCN support because they are well known for avoiding the formation of metal silicide as well as carbon nanotubes during ceramization. The

samples were characterized mainly by Thermo gravimetric analysis (TGA), powder X-ray diffraction (WXRD), nitrogen physisorption, TEM and SEM.

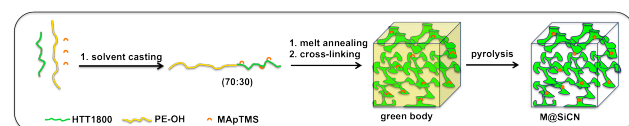


Figure 4. The synthetic route to metal containing mesoporous SiCN support.

The yield of the pyrolysed samples was calculated from thermo gravimetric analysis (TGA) curve. Increased yield was observed with the samples containing metal nanoparticles, which is due to the addition from the aminopyridinato complex (SI-Eqn.1 and 2). Powder X-ray diffraction analysis was performed to study both the green-body and pyrolysed metal nanoparticles containing SiCN materials. Primarily, the presence of metal nanoparticles at the amorphous SiCN support was substantiated. This analytical tool was also used to confirm the presence of amorphous and crystalline nature of PCCP and PE-OH blocks present in green body (Fig. SI-8). Both the Au@SiCN and Ag@SiCN catalysts is shown strong reflections ($\theta = 19, 22, 32, 38.5^\circ$) corresponding to the fcc planes [(111), (200), (220), and (331)] of Au & Ag nanoparticles immobilized on amorphous SiCN support (Fig. 1.d and SI. Flg. 4). The Debye-Scherrer equation was employed to 111 (FWHM = 2.1°) reflection peak for the measurement of an approximate size of 4.1 nm of the Au nanoparticles (SI. Fig. 6). Debye-Scherrer equation was employed to 111 (FWHM = 2. 1°) reflection peak for the measurement of approximate size of the nanoparticles exist in the catalysts and determined as 4.1 nm for the Au and 7.0 nm for Ag nanoparticles. The presence of smaller sized nanoparticles in the sample implies that the sintering of particles is successfully prevented.

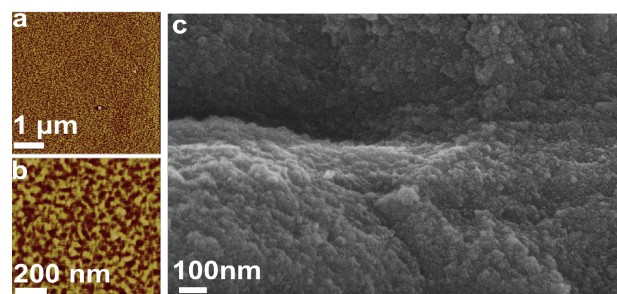


Figure 5. a-b. AFM images (non-tapping mode) of crosslinked PEOHTT-2 greenbody **c.** SEM image showing surface morphology of SiCN-2 ceramics.

Green body of SiCN-2 was studied with AFM (Atomic Force Microscopy) to understand the surface morphology before the pyrolysis. AFM technique is more appropriate to monitor the structure in green body stage because of its insolubility to solvents and poor withstanding nature (organic block) to electron beam. After performing non- tapping AFM mode on the surface of the greenbody, a new type of morphology for PEOHTT-2 is confirmed (Figure 7. a, b). Upon pyrolysis, the

surface morphology of SiCN-2 was investigated primarily using SEM (Surface Electron Microscopy) to confirm the retention of morphology (Figure 7. c). Afterwards, mesoporous nature of the SiCN-2 sample was examined using TEM (Transmission Electron Microscopy) and the mesoporous nature was revealed (Figure 7. d, e). The collective result from both SEM and TEM implies that the nature of the sample is porous as well as mesostructured. Metal nanoparticles supported mesoporous SiCN was analyzed mainly by TEM (Figure 10) and corroborate that these metal nanoparticles immobilized on the mesoporous SiCN support. Size of the particles observed by TEM image was further confirmed by recording WXRD of the sample. Difference of particles size observed by TEM and calculated by Debye-Scherrer equation of (111) reflection was 4 ± 2 nm (fig 9 and SI-7).

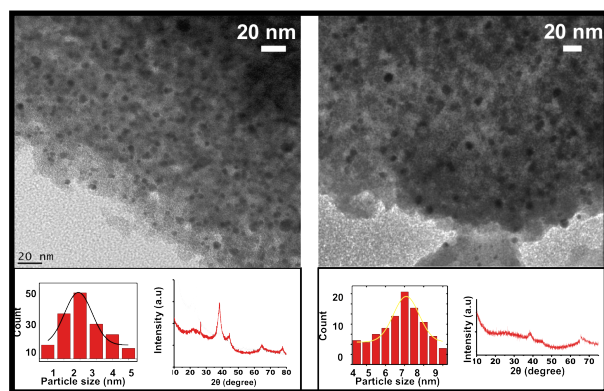


Figure 7. Representative TEM image of Au@SiCN (left) and Ag@SiCN (right) and inset of respective particle size distribution with powder XRD reflection pattern.

Histogram of the manually calculated particles was created and Gaussian distribution was applied to calculate the median size of the nanoparticles. Ag-SiCN samples were analyzed and presence of nanoparticles is confirmed. Interestingly, graphitic phase was not observed with Ag-SiCN samples. The size of the nanoparticles observed in Ag-SiCN is bigger than observed in Au-SiCN sample.

Nitrogen adsorption studies were carried out to understand the textural properties of mesoporous SiCN and metal particles integrated mesoporous SiCN materials. Type IV isotherm was observed on SiCN-1 (PEOHTT-1), SiCN-2 (PEOHTT-2), Au-SiCN (PEOHTT-Au), and Ag-SiCN (PEOHTT-Ag) samples. Whereas, SiCN-3 (UniOHTT-1), SiCN-4 (UniOHTT-2) samples shown type II isotherm. First, we wanted to study the samples pyrolysed with having different weight fraction of pore generating block in the samples. Sample SiCN-1, having 30% of PE block, exhibits with surface area of $117\text{ m}^2/\text{g}$ and pore volume of 0.124 cc/g . whereas, the highest BET surface area of $460\text{ m}^2/\text{g}$ was observed for SiCN-2, having 70% of PE block, with pore size distribution that solely belongs to mesoscale (9.414 nm). The large quantity of void space was substantiated from the calculated adsorbed pore volume of $0.553\text{ cm}^3/\text{g}$. This implies that increasing the weight fraction of PE introduces large quantity of void space in the sample that leading to the highest surface area. Secondly, we were curious to know if the length of the alcohol brings any changes in the pore size.

Interestingly, Sample SiCN-4, having 70% of unilene alcohol, was observed to have pores predominantly in microscale with total BET surface area of $383\text{ m}^2/\text{g}$ and pore size distribution of 1.379 nm . Furthermore, de Boer method^[19] was employed to figure out the contribution of surface area belongs to micropores (S_{micro}) from total BET surface area. Calculated surface area belongs to micropores by de Boer method was of $328\text{ m}^2/\text{g}$ with micropore volume of $0.166\text{ m}^2/\text{g}$. A critical evaluation using statistical thickness plot (t -plot)^[20] was performed to understand more about the porous nature of SiCN-2 and SiCN-4 samples. Interestingly, calculated positive intercept for SiCN-4 sample and negative intercept (extrapolated to zero) for SiCN-2 confirms the presence of micropores in SiCN-4 (fig.7) sample. Thirdly, we tried to introduce nanoparticles to understand the changes in textural properties of the resultant material.

The synthesized Au-SiCN with nanoparticles have shown $303\text{ m}^2/\text{g}$ in mesoscale. Comparing with SiCN-2 sample, smaller pore size distribution (8.145 nm) and reduced amount of adsorbed volume ($0.350\text{ cm}^3/\text{g}$) are noticed. Pore size distribution curve showing two different distributed peaks for these samples confirms to have mesoporous structure. We also extended this study to silver nanoparticles supported mesoporous SiCN system. Inference was that the mesoporous SiCN containing metal nanoparticles shown both the surface area and adsorbed pore volume less than observed for the SiCN-2 sample (table.1). Difference of surface area with in the metal particles embedded SiCN samples, Au-SiCN and Ag-SiCN, is based on the size of the nanoparticles blocking the pores as well as surface energy of the respective metal nanoparticles. For instance, Au-SiCN with highest surface area ($303\text{ m}^2/\text{g}$) accounts to the smaller size of the gold nanoparticles.

Table 1. Summery of textural properties of synthesized materials.

| Sample ID | P E : HTT ^a | Surface area (m^2/g) | | Pore size distribution (nm) ^b | Classification ^c | Pore volume (cc/g) | |
|-----------|---------------------------|---|--------------------|---|-----------------------------|----------------------------------|--------------------|
| | | S_{BET} | S_{micro} | | | V_{DFT} | V_{micro} |
| SiCN-1 | 30 : 70 | 117 | 0.000 | 9.316 | meso | 0.124 | 0.000 |
| SiCN-2 | 70 : 30 | 460 | 6.3 | 9.414 | meso | 0.553 | 0.000 |
| SiCN-Au | 70 : 30 | 303 | 0.000 | 8.145 | meso | 0.350 | 0.000 |
| SiCN-Ag | 70 : 30 | 257 | 0.000 | 8.123 | meso | 0.338 | 0.000 |
| SiCN-3 | 30 : 70 | 236 | 220 | 1.289 | meso & micro | 0.204 | 0.130 |
| SiCN-4 | 70 : 30 | 383 | 328 | 1.379 | meso & micro | 0.236 | 0.166 |

^a Weight ratio, ^b Calculated by density functional theory (DFT), ^c Mesopore size distribution curve and volume histogram were used, S_{BET} -Surface area calculated by Brunauer-Emmett-Teller(BET) method, S_{micro} - Surface area belongs to micropores calculated by v-t (de Boer) method.

Conclusion

To the best of knowledge, microphases separated monolithic green body consist of copolymer of poregen block and precursor block is first time successfully analysed for the

confirmation of microphase separated morphology by using AFM. Copolymers by varying the length of Porogen and mass ratio with precursor block is synthesized and detailed study on influencing pore size, pore classification, and surface area of resultant SiCN is presented. The surface area of SiCN has been increased with changing the ratio of organic porogen block and subsequently pore size of the pyrolysed SiCN has been shifted from microscale to mesoscale as altering the length of the organic porogen block. The outcome of this study implies that the mesoporous SiCN with high surface area is obtained by higher weight ratio and lengthy porogen PE block by controlled pyrolysis of the green body morphologies at 1000°C. A robust polymer derived mesoporous SiCN supported gold and silver catalysts synthesised by using the *in-situ* concerted copolymer formation, microphase separation, and pyrolysis. An efficient version of hydroxyl terminated polyethylene block synthesised via Ziegler's Aufbaureaktion is used for the copolymer formation to attain fibrous morphology. The commercially available precursor block is used for the binding of gold and silver aminopyridinato metal complexes, precursor for gold and silver nanoparticles. Copolymer with organic and inorganic blocks containing metal precursor is a promising novel approach that ensure the outcome of support would lie in mesoscale and hence the metal nanoparticles. However, this approach needs to be implemented for the bulk synthesis (kg scale) with controlled porosity and size of the nanoparticles for the catalysis and battery anode applications.

Supporting Information

The authors have included the experimental part and cited additional references within the Supporting Information.

Acknowledgements

Financial support from the Deutsche Forschungsgemeinschaft, SFB 840, is gratefully acknowledged. Foremost thankful to Prof. Dr. R. Kempe for providing space in his laboratory to conduct all the experiments with friendly atmosphere and full freedom. Our sincere thanks to Dr. Winfried P. Kritschmer for the PE-OH part. We thank Justus Hermannsdörfer for recording the TEM images, Dr. Wolfgang Milius for XRD studies and Renee Siegel for recording the MAS NMR spectra. We also thank Sandra Ganzleben for TGA measurements and Dr. Muhammed Zaheer for the compilation and date analysis. Supporting Information is available online from Wiley Inter Science or from the author.

Keywords: • Polymer Derived Ceramics • Mesoporous SiCN catalyst • Mesostructured SiCN • Supported Catalyst

References

- [1] P. Colombo, R. Riedel, G. D. Soraru, H. -J. Kleebe (Eds). *Polymer Derived Ceramics: From Nano-Structure to Applications*. D. E. Stech, Publications Inc., Lancaster USA **2010**. b) P. Colombo, G. Mera, R. Riedel, G. D. Soraru, *J. Am. Ceram. Soc.*, **2010**, 93, 1805–1837.
- [2] a) D. R. Rolison, Catalytic Nanoarchitectures—the Importance of Nothing and the Unimportance of Periodicity, *Science* 2003, 299, 1698-1701.
- [3] a) M. Zaheer, T. Schmalz, G. Motz, R. Kempe, Polymer derived non-oxide ceramics modified with late-transition metals, *Chem. Soc. Rev.* 2012, 41, 5102–5116..
- [4] M. Kamperman, A. Burns, R. Weissgraeber, N. van Vugten, S. C. Waren, S. M. Gruner, A. Balken, U. Wiesner, Integrating structure control over multiple length scales in porous high temperature ceramics with functional platinum nanoparticles, *Nano. Lett.* **2009**, 9 (7), 2756-2762
- [5] M. Zaheer, C. D. Keenan, J. Hermannsdörfer, E. Roessler, G. Motz, J. Senker, R. Kempe, Robust Microporous Monoliths with Integrated Catalytically Active Metal Site Investigated by Hyperpolarized ¹²⁹Xe NMR. *Chem. Mater.* **2012**, 24, 3952-3963..
- [6] a) W. M. Deen, M. P. Bohrer, N. B. Epstein, Effects of Molecular Size and Configuration on Diffusion in Microporous Membranes, *AIChE J.* 1981, 27, 952-959. b) J. Kärger, D. Freunde, Mass Transfer in Micro- and Mesoporous materials. *Chem. Eng. Technol.* 2002, 25(8), 769-778. c) R. Schlögl, Theory in heterogeneous catalysis an experimentalist's view, *CATTECH* 2001, 5(3), 146-170.
- [7] J.-K. Ewert, C. Denner, M. Friedrich, G. Motz, R. Kempe, Meso-Structuring of SiCN Ceramics by Polystyrene Templates. *Nanomaterials* **2015**, 5, 425-435. <https://doi.org/10.3390/nano5020425>.
- [8] Q. D. Nghiem, D. Kim, and D. -P. Kim, Synthesis of Inorganic–Organic Diblock Copolymers as a Precursor of Ordered Mesoporous SiCN Ceramic, *Adv. Mater.* **2007**, 19, 2351–2354.
- [9] a) M. C.Orilall, U. Wiesner, Block copolymer based composition and morphology control in nanostructured hybrid materials for energy conversion and storage: solar cells, batteries, and fuel cells, *Chem. Soc. Rev.* 2011, 40, 520-535. c) F. H. Schacher, P. A. Rupar, I. Manners, Functional Block Copolymers: Nanostructure Materials with Emerging Applications, *Angew. Chem. Int. Ed.* 2012, 51, 7898 – 7921. d) Y. Wang, F. Li, An Emerging Pore-Making Strategy: Confined Swelling-Induced Pore Generation in Block Copolymer Materials. *Adv. Mater.* 2011, 23, 2134-2148.
- [10] S. K. T. Pillai, W. P. Kretschmer, C. Denner, G. Motz, M. Hund, A. Fery, M. Trebbin, S. Förster, R. Kempe, SiCN Nanofibers with a Diameter Below 100 nm Synthesized via Concerted Block Copolymer Formation, Microphase Separation, and Crosslinking. *Small* 2013, 9(7), 984-989.
- [11] S. K. T. Pillai, W. P. Kretschmer, M. Trebbin, S. Förster, R. Kempe, Tailored Nanostructuring of End-Group-Functionalized High-Density Polyethylene Synthesized by an Efficient Catalytic Version of Ziegler's "Aufbaureaktion",, *Chem. Eur. J.* 2012, 18, 13974-13978.
- [12] J. H. de Boer, B. C. Lippens, B. G. Linsen, J. C. P. Broeckhoff, A. van den Heuvel, T. V. Onsinga, The t-curve of multimolecular N₂-adsorption. *J. Colloid Interf. Sci.* 1966, 21, 405-414.
- [13] B. C. Lippens, J. H. de Boer, Studies on pore systems in catalysis : V. The t method, *J. Catal.* 1965, 4 (3), 319-413.
- [14] A. Corma, From Microporous to Mesoporous Molecular Sieve Materials and Their Use in Catalysis, *Chem. Rev.* 1997, 97, 2373.
- [15] a) G. Glatz, G. Motz, R. Kempe, *Z. Anorg. Allg. Chem.* 2008, 634, 2897- 2902; b) R. Kempe, P. Arndt, *Inorg. Chem.* 1996, 35, 2644
- [16] a) Review of the anatase to rutile phase transformation, D. A. H. Hanaor, C. C. Sorrell, *J. Mater. Sci.* 2011, 46, 855-874. b) Y-S. Lin, C-H Chang, R. Gopalan, Improvement of Thermal stability of Porous Nanostructured Ceramic Membranes, *Ind. Eng. Chem. Res.* 1994,

33, 860-870. c) M. Veith, A. R. Lupini, S. Rashkeev, S. J. Pennycook, D. R. Mullins, V. Schwartz, C. A. Bridges, N. J. Dudney, thermal stability and catalytic activity of gold nanoparticles supported on silica, *J. Catal.* 2009, 262, 92-101.

[17] a) C. T. Campbell, S. C. Parker, D. E. Starr, The Effect of Size-Dependent Nanoparticle on Catalyst Sintering, *Science* 2002, 298, 811-814. b) P. Wynblatt, N. A. Gjostein, Supported metal crystallites, *Prog. Solid State Chem.* 1975, 21, 9-58. c) Ph. Buffat, J. -P. Borel, size effect on the melting temperature of gold particles, *Phys. Rev. A*. 1976, 13, 2287-2298.

[18] a) Y. Shi, Y. Wan, D. Zhao, Ordered mesoporous non-oxide materials, *Chem. Soc. Rev.* 2011, 40, 3854-3878. b) E. Ionescu, H. -J. Kleebeeb, R. Riedel, Silicon-containing polymer-derived ceramic nanocomposites (PDC-NCs): preparative approaches and properties, *Chem. Soc. Rev.* 2012, 41, 5032-5052.

[19] J. H. de Boer, B. C. Lippens, B. G. Linsen, J. C. P. Broeckhoff, A. van den Heuvel, T. V. Onsinga, The t-curve of multimolecular N₂-adsorption. *J. Colloid Interf. Sci.* 1966, 21, 405-414.

[20] B. C. Lippens, J. H. de Boer, Studies on pore systems in catalysis : V. The t method, *J. Catal.* 1965, 4 (3), 319-413.